MHD and Fluid Instabilities at the Plasma Edge in the Presence of a Separatrix and X-Point

J.R. Myra,[a] D.A. D'Ippolito[a], X.Q. Xu[b] and R.H. Cohen[b]

(a) Lodestar Research Corporation,
     Boulder CO 80301 USA
(b) Lawrence Livermore National Laboratory,
     University of California, Livermore CA 94550 USA

email: myra@lodestar.com

Abstract

The effect of an X-point and separatrix on unstable modes is considered within the context of MHD and fluid models. We begin by reviewing the magnetic flux geometry in the vicinity of the X-point and the effect it has on wave behavior. We then consider fluid models for the edge and SOL plasma based on the reduced Braginskii equations, and subsets thereof. For parameters typical of tokamak boundary plasmas, the models support a variety of low frequency instabilities including ideal and resistive MHD modes, drift-Alfven instabilities, and instabilities driven by sheath and neutral physics. The physics of these modes and the role of X-point geometry on them is elucidated. Recent results of turbulence simulations of the boundary plasma in X-point geometry are also discussed.

1   Introduction

The presence of a magnetic X-point and divertor is known experimentally to influence the tokamak boundary plasma and L-H transition. While the X-point and divertor influence many aspects of the boundary plasma equilibrium, one important effect, considered here, is the effect of the magnetic geometry on unstable modes and edge turbulence. In particular, along a field line the X-point introduces a region of strong magnetic shear, increased field line dwell and increased connection length. Radially, the separatrix divides the plasma into an interior region (referred to subsequently as the edge plasma) which has periodic (ballooning) boundary conditions (BCs), and a scrape-off-layer (SOL) region for which sheath boundary conditions apply at the divertor plates.

The scope of our review is limited to work either specifically treating edge instabilities in X-point geometry or work which highlights boundary plasma (edge and SOL) physics for which inferences about X-point effects may reasonably be made. We do not attempt a general review of tokamak edge turbulence here. Also excluded are thermal and axisymmetric (n = 0) modes which may be better treated in the context of X-point equilibria.

2 X-point geometry and wave physics

The magnetic geometry of a divertor tokamak is that of a poloidal field null with a strong superimposed toroidal field. The relevant Taylor expansion for vacuum fields is

$$\mathbf{B(x)} = \mathbf{B}_0 + \mathbf{x} \cdot \nabla B = B_z \mathbf{e}_z + \alpha \, (x \mathbf{e}_x - y \mathbf{e}_y), \tag{1}$$

which shows that all current-free X-points are locally equivalent up to scale factors. Equation (1) has been employed in Refs. [1] and [2] to investigate the resulting wave behavior. Before considering specific effects on particular modes of interest for edge turbulence, in this section we consider some general features.

The field line equations $dx/B_x = dy/B_y = dz/B_z$ can easily be integrated for B given by Eq. (1) and show that flux tubes near the separatrix which begin with circular cross section rapidly acquire a strong elliptical distortion [2] due to the magnetic shear of the X-point region. The field lines also linger poloidally near the X-point while traveling toroidally, and this results in an increased dl/B weighting of the X-point region [3] and in increased connection lengths [4]. Depending on the particular sensitivities of the mode in question, either of these effects can be dominant. In general, the increased field line length singularity is logarithmic in $|\mathbf{x}|$, while the global magnetic shear singularity is stronger because it is algebraic in $|\mathbf{x}|$ [5].

For axisymmetric systems, the toroidal mode number n of a wave perturbation may be specified. In the eikonal approximation, taking the usual drift/ballooning ordering $\mathbf{k} \cdot \mathbf{B} = 0$ in leading order, one obtains an X-point singularity in $k_\theta = nB/RB_p$ [6, 7]. The eikonal representation [$\mathbf{k} = \nabla S$ hence $\nabla \times \mathbf{k} = 0$] leads to an integral for k_ψ [7, 8] controlled by magnetic shear, as usual in the ballooning formalism. The magnetic shear effect of the X-point, however, is dramatic and quantitatively unlike the shear effect present for tokamaks without a separatrix. The rapid growth of k_ψ along a field line passing near the X-point may be viewed as arising from the strong squeezing deformation of the flux tubes which can be chosen to represent equiphase contours of a wave [2]. The enhancements of both k_θ and k_ψ give rise to enhancements of $k_\perp^2$ which can easily exceed an order of magnitude, for a single pass at distances of several ion Larmor radii from the X-point. Thus, the increased importance of effects proportional to $k_\perp^2$ such as ion finite Larmor radius effects (FLR), electron resistivity and inertia, near the X-point can be anticipated. One effect of an X-point is therefore to decouple field line regions on either side of it, e.g. the main SOL from the divertor BCs [2].

Analysis of model drift wave [6] and reduced MHD [7] equations show that the eikonal solution can break down near the separatrix and X-point. However, as we shall see, a variety of physical effects such as resistivity, FLR and the increase in mode damping due

to electron thermal diffusivity $\chi_\parallel$ that enters as $k_\parallel$ increases [9], often causes modes to avoid the X-point region.

Numerical work that is free of the eikonal assumptions is being pursued from several approaches [9-12]. However, the eikonal theory provides a useful conceptual framework in which many important physical issues may be addressed.

3   Fluid models for instability and turbulence studies

In Secs. 4 - 7 we will consider the effects of X-points on specific types of modes. For this purpose, it is useful to have in mind a physics model. We consider here the reduced collisional Braginskii fluid model [13, 14] (a compressional drift-resistive extension of MHD) and subsets thereof. Equations for vorticity (charge conservation), Ohm's law, continuity, electron and ion energy, Amperes law, and parallel mass flow yield respectively the electrostatic potential ϕ, parallel current $J_\parallel$, density n_e, species temperatures T_e and T_i, vector potential $\mathbf{A} = A_\parallel \mathbf{b}$, and parallel velocity $u_\parallel$.

Some important characteristic frequencies and dimensionless parameters of the model are as follows: the Alfven frequency $\omega_a = v_A/R$, the diamagnetic frequencies $\omega_{*j} = \mathbf{k} \cdot \mathbf{v}_{dj}$ ($j = i, e$), $\omega_\kappa = (2c(T_i+T_e)/eB) \, \mathbf{k} \cdot \mathbf{b} \times \kappa$ where κ is the curvature, the MHD drive term $\gamma_{mhd}^2 = -(\omega_\kappa(\omega_{*e}-\omega_{*i})/k_\perp^2 \rho_s^2(1+T_i/T_e))$, $H = k_\perp^2 c^2/\omega_{pe}^2$ which determines the importance of electron inertia, the resistive frequency $\omega_\eta = \eta_\parallel k_\perp^2 c^2/4\pi = H\nu_e$, and the ideal ballooning parameter $\alpha = \gamma_{mhd}^2 q^2 R^2/v_A^2$.

4   MHD and resistive MHD modes

The shear Alfven wave dispersion relation is $\omega^2 = (\mathbf{k} \cdot \mathbf{b})^2 \, v_A^2$. Since ω is conserved for time-independent equilibria, there is a tendency for a component of $\mathbf{k}$ to become large when the corresponding component of $\mathbf{b}$ vanishes. This leads to rapid variations of $\delta\phi$ for an ideal shear Alfven wave approaching the separatrices [7]. The perturbed current $\delta J_\parallel$ is proportional to $k_\perp^2 \, \delta\phi$, thus singular current sheets along the separatrix lines, and especially near the X-point, are to be expected for ideal modes [1]. The coupling of shear Alfven waves to magnetosonic modes ($\omega^2 \sim k^2 \, v_A^2$) is weak for an X-point with a strong superimposed B_0 [1] because the frequency separation of the shear and compressional modes remains large. Consequently, it is adequate to restrict attention for MHD instabilities to the shear-Alfven branch.

Bishop [3] has analyzed ideal pressure driven ballooning modes ($n \to \infty$) in separatrix geometry to determine the effect of the X-point . The analysis considered the stability of a reference surface just inside the separatrix, and employed a local equilibrium solution to the Grad-Shafranov equation, valid the neighborhood of the reference surface. It was found that

increased global shear and increased connection length are not as important as the field line dwell effect, and hence whether the X-point is located in a good or bad curvature region. Finite equilibrium $J_\parallel$ on the reference surface was shown to have a stabilizing effect because it moves the zeroes of local shear (where ballooning modes like to localize) to regions of good curvature.

When the X-point is in a region of neutral or good curvature and the plasma is near or above its ideal first stability ballooning limit ($\alpha > \alpha_{crit} \sim 1$, as is frequently the case for H-mode pedestals), the eigenfunctions can balloon strongly in the bad curvature region, avoiding the X-point region. (As discussed later, ballooning can also occur due to resistive effects, in which case similar remarks apply.) Consequently, in this case, the effects of X-point geometry are expected to be minimal, and edge turbulence calculations in circular geometry [15] should apply, at least qualitatively.

When the ideal modes are stable, resistive instabilities must be considered. Wilson [16] extended Ref. [3] to the resistive ballooning mode case using the Δ' formalism (i.e. the slow resistive mode [17]). The Δ' formalism is best suited to low-n resonant modes where there is an ideal and a resistive region (the outer and inner layer in a radial analysis). In the extended ballooning coordinate θ this implies a two scale analysis ($\theta \sim 1$ and $\theta \gg 1$) where the long scale $\theta \gg 1$ has both an ideal region $\theta \ll \theta_r$ and a resistive region $\theta_r \ll \theta$. The drive for the mode comes from the ideal region and the condition for instability is $\Delta' > \Delta'_c$ where Δ'_c is a positive critical (threshold) value. Typical behavior of Δ' vs. the ballooning parameter α is that Δ' starts out at 0 for $\alpha = 0$ (when equilibrium current gradients are neglected) and increases up to infinity at the critical α for ideal instability. It was found [16] that when Δ'_c is sufficiently large and the X-point is in a good curvature region there is a significant region of stability to slow resistive modes near the separatrix.

For realistic edge parameters the large shear near the X-point makes it difficult to satisfy the conditions required for the separation of scales between the ideal and resistive regions: except for very low mode numbers, the modes tend to become resistive as soon as they pass the X-point. Thus the asymptotic ballooning mode analysis is not a generally useful tool: the modes in this limit become fully two-dimensional. Several approaches are possible for treating this situation. An asymptotic analysis of the resistive equations in the vicinity of X-point was carried out in Ref. [18], generalizing the Δ' formalism to the two-dimensional X-point case. The analysis was applied to current-driven modes and yielded slowly growing instabilities, compared to the more rapid ones in the resonant magnetic surface (1D) case.

A direct numerical solution of the compressional resistive reduced MHD equations

(including the sound wave) in separatrix geometry was obtained by Strauss [12]. These simulations of pressure driven ELMs with n ~ 1 - 4 displayed poloidal flow spin-up arising from the poloidally asymmetric transport-induced by the ballooning mode. The simulations also showed turbulence-generated mass flow into the divertor legs from the ELM events.

The β limits of divertor plasmas against low-n pressure driven external kink modes were examined in Ref. [10] using the KINX code. Plasma pressure profiles which have gradients peaking on the separatrix and current flowing in the SOL were considered with two types of BCs, that may be characterized as fixed (line tied) and free (similar to insulating). For a pressureless and currentless SOL, stability properties are similar to the non-diverted plasma case [10, 11] . Thus the separatrix itself has little effect. With plasma pressure and current in the SOL the fixed BC is strongly stabilizing while the free BC causes the β_n limit to drop [10].

The radially localized moderate- to high-n limit of the current-driven external kink mode is the peeling mode [19, 20]. Because the peeling mode is sensitive to the location of resonant magnetic surfaces with respect to the plasma edge, separatrix geometry is expected to have important consequences. Peeling mode studies so far include circular or moderately shaped cross-sections [19, 20] where the coupling to the ballooning mode plays a crucial role. Although some global simulations in X-point geometry have been carried out [21], a comprehensive understanding of the peeling mode in the presence of a separatrix and divertor remains an important topic for future work.

Returning to pressure driven modes and resistive ballooning stability, at moderate to high n we have noted that the Δ' formalism is invalid. However, in this regime a second type of resistive ballooning mode arises that is driven by β in the resistive region (rather than Δ' in the ideal region), viz. the fast resistive mode [17]. The earliest treatment [5] of this mode included X-point effects invoking the two-space scale ordering. In the extended ballooning angle θ, the mode varies on the scale $\theta \sim 1$. These rapid variations are modulated by a slow envelope extending to $\theta \gg 1$ that decays resistively. In this limit, the X-point geometry is averaged over by the envelope, and does not play a novel role in the mode behavior. The increased global shear inherent near the separatrix does exert a stabilizing influence on the mode [5].

As mode number n, resistivity and/or β increase, the fast resistive mode evolves to the point where the two-space scale ordering breaks down [22], i.e. the envelope varies on a scale $\Delta\theta \sim 1$. This ordering is normally the most relevant one near the separatrix when n is large enough to invoke the ballooning formalism. The fast resistive mode is unstable in this ordering when $\alpha \sim 1$, although instability can pertain well below the ideal boundary $\alpha =$

α_{crit}. The relevant strong-shear unstable branch of the resistive mode spectrum has been shown to connect to the ideal strong ballooning branch in the circular flux surface case [23]. Estimating the growth rate to be on the order of the ideal one $\omega \sim \gamma_{mhd}$ (hence the nomenclature *fast*), resistivity is expected to be important when $\omega \sim \omega_\eta \propto k_\perp^2 \eta_\parallel$. This can occur because the mode number n is large (classical resistive ballooning mode), or because the X-point geometry leads to a large enhancement of $k_\perp$ even though n is moderate (resistive X-point mode). We will consider unstable spectra which illustrate these distinct possibilities in Sec. 7 in the context of the full drift-resistive reduced Braginskii equations.

The resistive ballooning modes most commonly studied in the literature for circular tokamaks correspond to either the high-n variety of mode and/or to the two-space scale limit, where the mode is very extended in θ. In either case, the characteristic radial wavenumber k_r is very high, and this generally results in negligible radial diffusion coefficients [24] since the mixing length estimate is $D \sim \gamma/k_r^2$. Even the lowest mode number slow resistive instabilities do not circumvent this, because for them the growth rate becomes small, $\gamma = \text{Im}(\omega) \ll \gamma_{mhd}$. X-point geometry allows a new possibility: fast growing resistive instabilities at moderate n.

5 Drift type instabilities

The characteristic wavenumber for which resistivity affects MHD mode behavior is given from $\gamma_{mhd} \sim \omega_\eta$, where we henceforth assume a fast resistive mode ordering with $\alpha \sim 1$. Using the n^2 scaling of ω_η, one can derive a characteristic $n = n_r$ beyond which the modes are resistive. For $n \geq n_r$ it is frequently the case that drift effects are important, viz. $\omega_* \sim \gamma_{mhd}$, where $\omega_* \propto n$. The ion drift terms ω_{*i} can lead to FLR stabilization of MHD modes, while the electron terms ω_{*e} introduce the electron drift wave. In X-point geometry, drift effects are important relative to resistive effects even though $\omega_\eta \propto k_\perp^2$ is enhanced near the X-point while $\omega_* \propto k_\theta \partial/\partial\psi$ is constant along a field line when n, T_j are flux functions.

Drift instabilities have a long history in the tokamak turbulence literature, and early investigations into the effects of an X-point focused on electrostatic collisionless drift wave models appropriate to the universal and η_i modes [25, 26]. Applying an X-point model similar to that employed previously for the ideal [3] and resistive [16] MHD studies, the stability of the toroidicity induced drift wave was shown to depend on the location of the X-point [25] much as before, but for different reasons. With X-points on the inboard or outboard midplane, shear damping was found to be more inhibited than in the circular plasma case. In contrast, when the X-points were located at the top or bottom of the torus outward energy convection was found to be enhanced leading to greater mode stability.

Reference [25] notes a new branch of drift wave localized near the X-point, when a field line near the separatrix is considered. The η_i mode was considered in Ref. [26] where it was shown that in the steep density gradient case most relevant to edge plasmas, stability was dominated by curvature effects, and hence greater instability was found with X-points in the bad curvature region.

Typically, boundary plasmas are best described by electromagnetic semi-collisional or collisional models, where the η_i mode is frequently overshadowed by the resistive ballooning mode [27] and drift instabilities must be treated in the context of a drift-Alfven model [28, 29]. The basic drift-Alfven coupling is illustrated from the homogeneous plasma dispersion relation which can be written in the form

$$(\omega^2 - k_\parallel^2 v_a^2) \, [\omega(1+k_\perp^2\rho_s^2)-\omega_{*e}] = -\omega^2 \, (\omega H + \omega_\eta - \omega k_\perp^2\rho_s^2) \tag{2}$$

showing the factors for the two Alfven modes and the drift wave on the lhs, and coupling introduced by electron inertia , resistivity and ion FLR effects, respectively, on the rhs. The first two effects on the rhs give instability drives. Further analysis reveals that maximum growth typically occurs near mode crossing, i.e. $\omega \approx k_\parallel v_a \approx \omega_{*e}/(1+k_\perp^2\rho_s^2)$. Recent investigations of the drift-Alfven mode highlight its possible role in the physics of the L-H transition [29].

Past investigations have not specifically addressed the role of an X-point on the drift-Alfven mode. It can be argued that the basic physics of the drift-Alfven instability should not be much modified by separatrix geometry. An equation like Eq. (2) applies (as a differential equation along the field line) and since ω_{*e} is constant along a field line, the mode number n is still determined by the resonance condition $k_\parallel v_a = \omega_{*e}$. The differential equation determines $k_\parallel$ as a spectrum of discrete quantized values. The X-point region allows smaller $k_\parallel$ than in a similar circular plasma, due to the increased connection length effect, but only by a modest logarithmic factor of order 2 or 3. The main X-point effect is that $k_\perp$ grows dramatically along the field line, so that a localized region of significant drift-Alfven growth [driven by the rhs of Eq. (2) $\propto k_\perp^2$, when H ~ 1 or ω_η ~ ω] is usually encountered. Although not specifically an X-point effect, the radial mode structure and the validity of eikonal theory also warrant attention because the mode crossing condition $k_\parallel v_a = \omega_{*e}$ is typically satisfied at only one radial point.

6 SOL instabilities

In the SOL, the resistive X-point physics discussed prviously is still operative, but in addition the sheath BC that must be applied at the divertor plates permits new classes of instabilities (e.g. the ∇T_e sheath driven "conducting wall" mode [30]) and modifies the

stability of MHD curvature driven modes [4, 8, 31, 32]. These SOL-specific effects are discusssed here. In a limiter configuration the sheath BC is strongly destabilizing when it is in the insulating (free) and incomplete line tying BC limit, but strongly stabilizing when the BC is that of a perfect conductor (complete line tying) [31]. The transition is governed by the BC which matches the perturbed sheath current $\delta J_{\parallel sh} \sim n_e e^2 c_s\, \delta\phi/T_e$ to the current $\delta J_{\parallel s}$ of the Alfven or electrostatic resistive ballooning mode under consideration, at the sheath boundary (denoted by s). For Alfven waves the high-n limit is insulating since $\delta J_{\parallel a} \propto \nabla_{\parallel} k_\perp^2 \delta\phi$, and $\delta J_{\parallel sh} = \delta J_{\parallel s}$ implies $\nabla_{\parallel}\delta\phi_s = 0$ which is the free BC. In the opposite limit, e.g. for moderate and low-n modes, one obtains $\delta\phi_s = 0$ which is the line tied BC.

These considerations carry over to divertor configurations [4, 8]. The curvature drive in the SOL is naturally stronger than in the edge (just inside the separatrix) because the edge (SOL) region has good (bad) curvature near the X-point. When the SOL field line under consideration is sufficiently far from the separatrix, so that the connection length $L_{\parallel}$ is reduced, the effect of a line tying BC on ideal modes is stronger. A common feature that has emerged from two studies [4, 8] is that interchange-like modes are favored in X-point geometry, both because of the increased connection lengths and the sheath BCs (when they are in the insulating limit). Single and double null configurations behave differently because the average curvature in the latter case can be unfavorable in the SOL [32].

Although the ∇T_e sheath driven conducting wall mode can persist in X-point geometry [8], recent analysis for DIII-D suggests that this type of instability is not dominant [9], probably because of the decoupling of main SOL from the divertor BCs due to the X-point [2] and the stabilizing effect of shear between the X-point and the plates.

Neutral effects on instabilities in the SOL have also been studied in slab [33, 34, 35] and model X-point [36] geometries. Neutrals, which are coupled to the plasma through charge exchange, can drive an interchange-ballooning instability when the neutral pressure-gradient-driven flow is directed opposite to the plasma density gradient, but the conditions for this "ion-neutral drag" instability do not exist in normal divertor operation [33, 36]. The instability is sensitive to X-point effects on k_θ and k_ψ which control the relative contributions of the equilibrium $\partial/\partial\theta$ and $\partial/\partial\psi$ gradient drive terms [36]. Ion-neutral friction terms exert a stabilizing influence on ideal curvature driven modes but are less effective on resistive modes [36] because of X-point disconnection and the fact that the neutral population is normally localized near the divertor plates. A complete analysis of the effects of neutrals on plasma stability in X-point geometry including the effects of viscosity and cross field heat fluxes [34] is complicated by the difficulty in obtaining neutral-plasma equilibria when the mean free path limit is not short.

Space limitations preclude a discussion of other SOL instability mechanisms such as E×B shear [37, 8], parallel velocity shear [38] and SOL currents for which X-point effects have not been explicitly studied. A review of the status of SOL turbulence studies may be found in Ref. [39].

7 Turbulence simulations in X-point geometry

The nonlocal electromagnetic BOUT code has enabled 3D turbulence simulations in realistic divertor geometry including both the edge and SOL region [9, 40]. In combination with the linear eikonal BAL code [8] the linear and nonlinear behavior of modes described within the Braginskii model of Sec. 3. have been studied [9, 40]. A typical unstable spectrum from BAL is shown in Fig. 1 for DIII-D geometry on a flux surface 0.9 cm inside the separatrix ($\psi = 98\%$), with local L-mode edge parameters $n_e = 2.4 \times 10^{13}$ cm^{-3}, $T_e = 130$ eV, $T_i = 68$ eV, $L_n = 4.7$ cm, $L_{te} = 1.6$ cm, $L_{ti} = 3.8$ cm. The low-n spectral peaks around $n = 50$ ($\gamma = 1.2 \times 10^5$ s^{-1} corresponding to $\gamma/\gamma_{mhd0} = 0.15$ where 0 denotes the outboard midplane) are the resistive X-point modes discussed in Sec. 4. Eigenfunctions for this curvature-driven mode are somewhat interchange-like on the high-field-side of the torus, and decay to zero when they encounter the X-points; the electrostatic potential normally peaks near the X-point region where the mode transitions from being electromagnetic to electrostatic [9]. The high-n spectral peak in Fig. 1 is the classical resistive ballooning mode, which is more localized to the bad curvature at the outboard midplane.
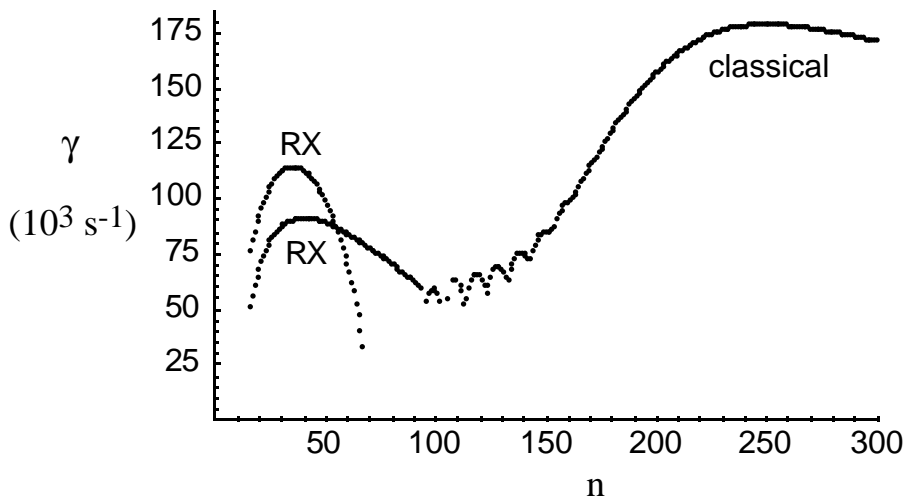
Fig. 1 Spectrum of unstable modes in the reduced Braginskii model, for parameters typical of the DIII-D edge plasma in L-phase.

While the instabilities in Fig. 1 are driven primarily by curvature, the drift-Alfven coupling discussed in Sec. 5 is also a contributing factor. When the curvature is artificialy set equal to zero, the maximum growth rate in Fig. 1 drops to $\gamma \sim 40 \times 10^3$ s^{-1}.

Heating of the local plasma occurs when these modes encounter the X-point dissipation region ($\omega \sim \omega_\eta$). When core heat sources are added to the BOUT simulations, the resistive MHD heating rate $Q_{mhd} = \eta_\| |J_\||^2/2$ is comparable to the parallel thermal conduction rate, and thus sufficient to drive a small localized increase in T_e at the X-point. These results are qualitatively consistent with recent experimental observations on DIII-D [41] where elevated temperatures have been observed in the L-phase on closed surfaces near the X-point. Theoretically, an interesting analogy between the X-point dissipation region and the dissipative wall boundary has been pointed out [42].

The strong enhancement of $k_\perp$ near the X-points calls into question the use of a fluid model (which assumes $k_\perp \rho_i < 1$) for the ion dynamics. For typical parameters $k_\perp \rho_i \sim 1$ pertains in the X-point region, where fortunately the modes begin to decay to zero. The BAL code has been employed to compare the linear results of the fluid model with a full gyrokinetic ion model. In the gyrokinetic model it is found that the highest n instabilities (see Fig. 1) are suppressed relative to the low-n branch, which acquires a broadened spectrum extending from below n = 40 to above n = 100. While the eigenfunctions for the fluid and gyrokinetic models differ in detail, they share some common features: the X-points tend to confine the modes, and the mode potential $\delta\phi$ is strongly peaked at the outboard side of the X-point region. Interestingly, with respect to suppression of the high-n modes, the BAL runs with the full gyrokinetic model show better qualitative agreement with BOUT than do the BAL fluid model runs. This may be due to the numerical (resolution limited) suppression of short-wavelengths in BOUT which acts like the $k_\perp \rho_i \sim 1$ physics.

BOUT simulations [9] of the DIII-D boundary plasma using experimentally measured n, T and Φ profiles in the L- and H-phases, held fixed in the code, show suppression of fluctuation levels and turbulent diffusivities in the H-phase. The ion diffusivities calculated from BOUT are comparable to those required in DIII-D UEDGE boundary plasma modeling and hence to those inferred from the experimentally measured profiles. The dynamic evolution of the L-H transition has recently been simulated in BOUT by incorporating simple sources near the core boundary and sinks in the SOL region [43]. An H-mode-like pedestal is formed with much reduced transport and a large negative radial electric field is established near the separatrix due to turbulence-generated plasma rotation.

8 Summary

The magnetic geometry near an X-point is shown to affect wave stability through three processes: increased magnetic shear, field line lingering near the X-point and increased connection length, $L_\parallel$. The null in B_p gives a local singularity in k_θ, and shear gives integrated growth of k_ψ. The resulting enhancement of $k_\perp$ causes decoupling of fluctuations along field lines that pass near the X-point for sufficiently high mode number waves, and in some cases can invalidate eikonal theory. For ballooning modes, stability is sensitive to the location of the X-point. When the X-point region has neutral curvature its presence is less significant in the strong ballooning limit ($\alpha \gg 1$ or high-n resistive). For high-n modes in the SOL, increased $L_\parallel$ and $k_\perp$ (combined with the effects of resistivity and FLR) tends to decouple the main SOL from the divertor region (boundary conditions and the effect of neutrals at the plate) making the edge and main SOL behave similarly. In contrast, low-n modes can propagate around the X-point, and thus can be influenced by the divertor plate boundary condition. The latter can be either stabilizing (line tied) or destabilizing (insulating or partially conducting). The increased magnetic shear near the separatrix is normally stabilizing for pressure-driven modes (at sufficiently low n to penetrate the X-point), and less consequential for global current-driven modes. Separatrix and X-point effects are expected to influence edge-localalized peeling modes, and to a lesser extent drift-Alfven modes, though at present the effects are not fully characterized.

In the moderate-n regime, there is an important class of interchange-ballooning modes associated with X-point geometry that are electromagnetic and curvature driven on the outboard side of the torus, and become electrostatic (due to resistive effects) near the X-point. These "resistive X-point modes" appear to dominate turbulence simulations which show encouraging agreement with experiment, viz. localized X-point heating, turbulence suppression in the H-phase and calculated ion thermal diffusivities on the order of experimentally deduced values.

Acknowledgments

References

[1] BULANOV, S.V., SHASHARINA, S.G., PEGORARO, F., Plasma Phys. Cont. Fusion **34** (1992) 33

[2] FARINA, D, POZZOLI, R., RYUTOV, D.D., Nucl. Fusion **33** (1993) 1315

[3] BISHOP, C.M., et al., Nucl. Fusion **26** (1986) 1063 ; Bishop, C.M., et al., Nucl. Fusion **12** (1984) 1579

[4] KERNER, W., POGUTSE, O., VAN DER LINDER, R., Plasma Phys. Cont. Fusion **39** (1997) 757

[5] HAHM, T.S., DIAMOND, P.H., Phys. Fluids **30** (1987) 133

[6] MATTOR, N., COHEN, R.H., Phys. Plasma **2** (1995) 4042

[7] MYRA, J.R., D'IPPOLITO, D.A., Phys. Plasma **5** (1998) 659

[8] MYRA, J.R., D'IPPOLITO, D.A., GOEDBLOED, J.P., Phys. Plasma **4** (1997) 1330

[9] XU, X.Q. et al., presented at the *17th IAEA Fusion Energy Conf.*, Yokohama, Japan, October 1998, paper IAEA-CN-69/THP2/03

[10] DEGTYAREV, MARTYNOV, A., MEDVEDEV, S., VILLARD, L., 24th European Phys. Soc. Conf. on Cont. Fusion and Plasma Phys. (Berchesgarten, 1997) Vol. 21A, Part II, p. 845

[11] LEE, J.K., Phys. Fluids **29** (1986) 1629

[12] STRAUSS, H.R., Phys. Plasma **3** (1996) 4095

[13] BRAGINSKII, S.I., in *Reviews of Plasma Physics*, edited by Leontovich, M.A. (Consultants Bureau, New York, 1965), Vol. 1, p. 205

[14] ZEILER, A., DRAKE, J.F., ROGERS, B., Phys. Plasma **4** (1997) 2134

[15] ROGERS, B.N., DRAKE, J.F, Phys. Plasma **6** (1999) 2797; and refs therein

[16] WILSON, H.R., Plasma Phys. Cont. Fusion **33** (1991) 221

[17] HAZELTINE, R.D., MEISS, J.D, Phys. Rep **121** (1985) 1

[18] DE BENEDETTI, M., PEGORARO, F., Plasma Phys. Cont. Fusion **37** (1995) 103

[19] WILSON, H.R., MILLER, R.L., Phys. Plasmas **6** (1999) 873

[20] CONNOR, J.W. et al.. Phys. Plasmas **5** (1998) 2687

[21] DEGTYAREV L., MARTYNOV A., MEDVEDEV S., TROYON F., VILLARD L., GRUBER R., Comp. Phys. Comm. **103** (1997), 10

[22] HENDER, T.C. et al., Phys. Fluids **27** (1984) 1439

[23] NOVAKOVSKII, S.V., GUZDAR, P.N., DRAKE, J.F., LIU, C.S., WAELBROECK, F.L., Phys. Plasmas **2** (1995) 781

[24] CARRERAS, B.A. et al., Phys. Rev. Lett. **50** (1983) 503

[25] BRIGUGLIO S., ROMANELLI, F., BISHOP, C. M., CONNOR, J. W., HASTIE, R.J., Phys. Fluids B **1** (1989) 1449

[26] BRIGUGLIO, S., Phys. Fluids B **3** (1991) 95

[27] ZEILER, A., BISKAMP, D., DRAKE, J.F., ROGERS, B.N., Phys. Plasmas **5** (1998) 2654

[28] JENKO, F., SCOTT, B., Phys. Plasmas **6** (1999) 2705

[29] POGUTSE, O., IGITHANOV, YU, KERNER, W., JANESCHITZ, G., CORDEY, J.G., 24th EPS Conf. on Cont. Fusion and Plasma Phys (Berchesgarten, 1997) Vol 21A, Part III, p. 1041; POGUTSE, O., IGITHANOV, YU, Czechoslovak J. Phys **48** Suppl. S2 (1998) 39

[30] BERK, H.L., COHEN, R.H., RYUTOV, D.D., TSIDULKO, YU. A., XU, X.Q., Nucl. Fusion **33** (1993) 263; and refs. therein

[31] NOVAKOVSKII, S.V., GUZDAR, P.N., DRAKE, J.F., LIU, C.S., Phys. Plasmas **2** 3764 (1995)

[32] KERNER, W., NASSIGH A., POGUTSE, O., Plasma Phys. Cont. Fusion **39** (1997) 1101; POGUTSE, O. et al. 21st EPS Conf. on Cont. Fusion and Plasma Phys (Montpellier, 1994) Vol 18B, Part II, p. 882

[33] DAUGHTON, W., COPPI, B., CATTO, P., KRASHENINNIKOV, S., Phys. Plasmas **5** (1998) 2217

[34] ODBLOM, A., CATTO, P., KRASHENINNIKOV, S., Phys. Plasmas **6** (1999) 3239

[35] XU, X.Q., COHEN, R.H., Plasma Phys. Cont. Fusion **35** (1993) 1071

[36] D'IPPOLITO, D.A., MYRA, J.R., Phys. Plasmas **6** (1999) 519

[37] TSIDULKO, YU. A., BERK, H.L., COHEN, R.H., Phys. Plasmas **1** (1994) 1199

[38] MCCARTHY, D.R., BOOTH, A.E., DRAKE, J.F., GUZDAR, P.N., Phys. Plasmas **4** (1997) 300

[39] XU, X.Q. AND COHEN, R.H., Contrib. Plasma Phys. **38** (1998) 158

[40] XU, X.Q., COHEN, R.H., PORTER, G.D., MYRA, J.R., D'IPPOLITO, D.A., MOYER, R., J. Nucl. Mat. **266-269** (1999) 993

[41] SCHAFFER, M.J. et al., Bull. Am. Phys. Soc. **43** (1998) 1889, paper R8P5

[42] RYUTOV, R., COHEN, R.H., Cont. Plasma Phys. **36**, (1996) 161

[43] XU, X., Q., invited paper, APS-DPP Conference, Seattle, WA, Nov.15-19, 1999; to be published in Phys. Plasmas